ORIGINAL ARTICLE

Arterial waveform morphomics during hemorrhagic shock

Philip J. Wasicek[1] · William A. Teeter[1] · Shiming Yang[1,2] · Peter Hu[1,2] · William B. Gamble[1] · Samuel M. Galvagno[2] · Melanie R. Hoehn[1] · Thomas M. Scalea[1] · Jonathan J. Morrison[1] 🔘

Abstract

Purpose The arterial pressure waveform is a composite of multiple interactions, and there may be more sensitive and specific features associated with hemorrhagic shock and intravascular volume depletion than systolic and/or diastolic blood pressure (BP) alone. The aim of this study was to characterize the arterial pressure waveform in differing grades of hemorrhage.

Methods Ten anesthetized swine (70–90 kg) underwent a 40% controlled exponential hemorrhage. High-fidelity arterial waveform data were collected (500 Hz) and signal-processing techniques were used to extract key features. Regression modeling was used to assess the trend over time. Short-time Fourier transform (STFT) was utilized to assess waveform frequency and power spectrum density variance.

Results All animals tolerated instrumentation and hemorrhage. The primary antegrade wave (P1) was relatively preserved while the renal (P2) and iliac (P3) reflection waves became noticeably attenuated during progressive hemorrhage. Several features mirrored changes in systolic and diastolic BP and plateaued at approximately 20% hemorrhage, and were best fit with non-linear sigmoidal regression modeling. The P1:P3 ratio continued to change during progressive hemorrhage ($R^2 = 0.51$). Analysis of the first three harmonics during progressive hemorrhage via STFT demonstrated increasing variance with high coefficients of determination using linear regression in frequency ($R^2 = 0.70$, 0.93, and 0.76, respectively) and power spectrum density ($R^2 = 0.90$, 0.90, and 0.59, respectively).

Conclusions In this swine model of volume-controlled hemorrhage, hypotension was a predominating early feature. While most waveform features mirrored those of BP, specific features such as the variance may be able to distinguish differing magnitudes of hemorrhage despite little change in conventional measures.

Keywords Trauma · Traumatic shock · Experimental hemorrhagic shock · Hemodynamic monitoring · Hemodynamic waveform analysis · Arterial waveform

Introduction

Understanding the cardiovascular response to hemorrhage is important as major bleeding constitutes the leading cause of preventable trauma death worldwide [1–3]. The most common description of hemorrhagic shock is presented by the American College of Surgeons, Advanced Trauma Life Support (ATLS) program, which classifies hypovolemia shock into classes I through IV. This is based upon the proportion of intravascular volume loss, with each class corresponding to specific clinical features and vital sign data [4]. While conceptually attractive with a sound physiological basis, several investigators have conducted pragmatic studies which do not support this doctrine [5–8].

This has led others to investigate more complex vital sign components in an effort to more reliably identify characteristics of hemorrhage [9–11]. The dynamic interaction of the heart forcefully ejecting blood into the compliant aorta and arterial tree results in an arterial pressure waveform that is the composite of these complex interactions. With worsening hemorrhage and hypovolemia, arterial waveform morphology may change depending on the severity of hypovolemia in more discrete ways than just systolic and diastolic blood pressure values. The arterial waveform has been previously

✉ Jonathan J. Morrison
jonathan.morrison@som.umaryland.edu

1   R Adams Cowley Shock Trauma Center, 22 S. Greene Street, Baltimore, MD 21201, USA

2   Shock Trauma and Anesthesiology Research Center, University of Maryland, School of Medicine, Baltimore, MD, USA

reported to change in a swine model of hemorrhagic shock (estimated blood volume loss 27%) secondary to alterations in major wave reflections in the aorta; however, it remains unclear if these changes are progressive and if the features can be associated with varying severities of hemorrhagic shock [10].

While the study of waveform morphology has largely focused on hypertension and other physiological states, the dynamic changes observed during hemorrhage have yet to be fully characterized. It may be the case that the understanding and application of these changes may lead to better methods of the identification of shock. The objective of this study was to employ advanced signal-processing techniques in a large animal traumatic hemorrhage model to better understand observable changes that occur in the arterial waveform during hemorrhagic shock.

Materials and methods

Study overview

This in vivo study characterizes the changes in arterial waveforms that occur during hemorrhage and uses Yorkshire swine (*Sus scrofa*) weighing between 70 and 90 kg. Once animals were induced into hemorrhagic shock, animals were subsequently enrolled into other studies, which will be reported separately, but the current study represents a detailed analysis of this common experimental phase. This has been conducted in this way, to reduce overall animal use, in adherence to the principles of the 3Rs (Replacement, Reduction, and Refinement).

Compliance with ethical standards

This study was undertaken at a certified laboratory, following Institutional Animal Care and Use Committee (IACUC) approval. The manuscript is compliant with the ARRIVE (Animal Research: Reporting of In Vivo Experiments) guidelines [12]. The study consisted of two phases: animal preparation and volume-controlled hemorrhage.

Animal preparation

General anesthesia was induced using intramuscular ketamine (10–15 mg/kg) and xylazine (1–2.2 mg/kg) followed by intravenous propofol and ketamine, and maintained with isoflurane (minimum alveolar concentration [MAC] range 1–4%) by mask followed by tracheostomy intubation. Animals were ventilated using a volume-controlled mode of 6 cc/kg with an FiO_2 of 40–100% to maintain $SpO_2 > 92\%$.

Surgical exposure via a midline neck incision was performed to permit cannulation of the common carotid artery with a 5 Fr high-fidelity solid-state pressure sensor (Transonic Sciences Pressure Catheter, Transonic Systems Inc., Ithaca, NY, USA), which was advanced into the aortic arch. The contralateral carotid artery was also exposed enabling the placement of a flow probe (FSB-Series, Transonic Systems Inc., Ithaca, NY, USA). The jugular veins were also cannulated bilaterally to permit intravenous access and placement of a Swan–Ganz catheter. The right femoral vein also cannulated via a cut-down to permit venesection. An open cystostomy was performed for urine drainage.

Volume-controlled hemorrhage

Hemorrhagic shock was induced using a standardized technique as previously described [13]. Assuming a porcine blood volume of 66 mL/kg, 40% of the animal's blood volume was removed over the course of 20 min from the femoral venous catheter. The first 20% of blood volume was removed over 7 min, and the remaining 20% of blood volume was removed over 13 min.

To prevent hemorrhage-induced cardiac arrest, animals were bolused up to 3×500 mL of lactated ringers, if in the judgement of the anesthetist, the animal was close to arrest. The animals were euthanized at the end of the protocol, and the pressure catheter tip location was confirmed to be in the aortic arch at necropsy.

Arterial waveform data processing and statistical analysis

Arterial waveform data were recorded continuously throughout the experiment and signal processing was performed using MATLAB (MathWorks Inc., Natick, MA, USA). The arterial waveform is a wavefront composed of several waves, either produced by cardiac contraction or reflection off the distal arterial tree [9, 14]. While there are numerous and complex interactions in this hydraulic system, the arterial waveform can be considered to consist of three major waves (Fig. 1a). P1 represents the primary antegrade systolic peak, P2 the first wave reflection at the level of the renal arteries, and P3 represents the iliac wave reflection.

The first and second derivatives of the waveform were used to extract key features which correspond to inflection points, nadirs, and zeniths (Fig. 1b). These data were analyzed as continuous data to measure the rates of change in the amplitude of key features during hemorrhage (Fig. 1b). Linear and non-linear (sigmoidal) regression modeling were used to quantify trends and strength of associations.

Fourier transform was utilized as an additional method of analyzing the arterial waveform during progressive hemorrhage. Fourier transform allows quantification and measurement of the differing frequencies and waves that compose the wavefront of the arterial waveform. This is accomplished

Fig. 1 **a** Illustration of arterial waveform with three main wave components. **b** Key arterial waveform features. *P1* primary wave reflection, *P3* iliac wave reflection
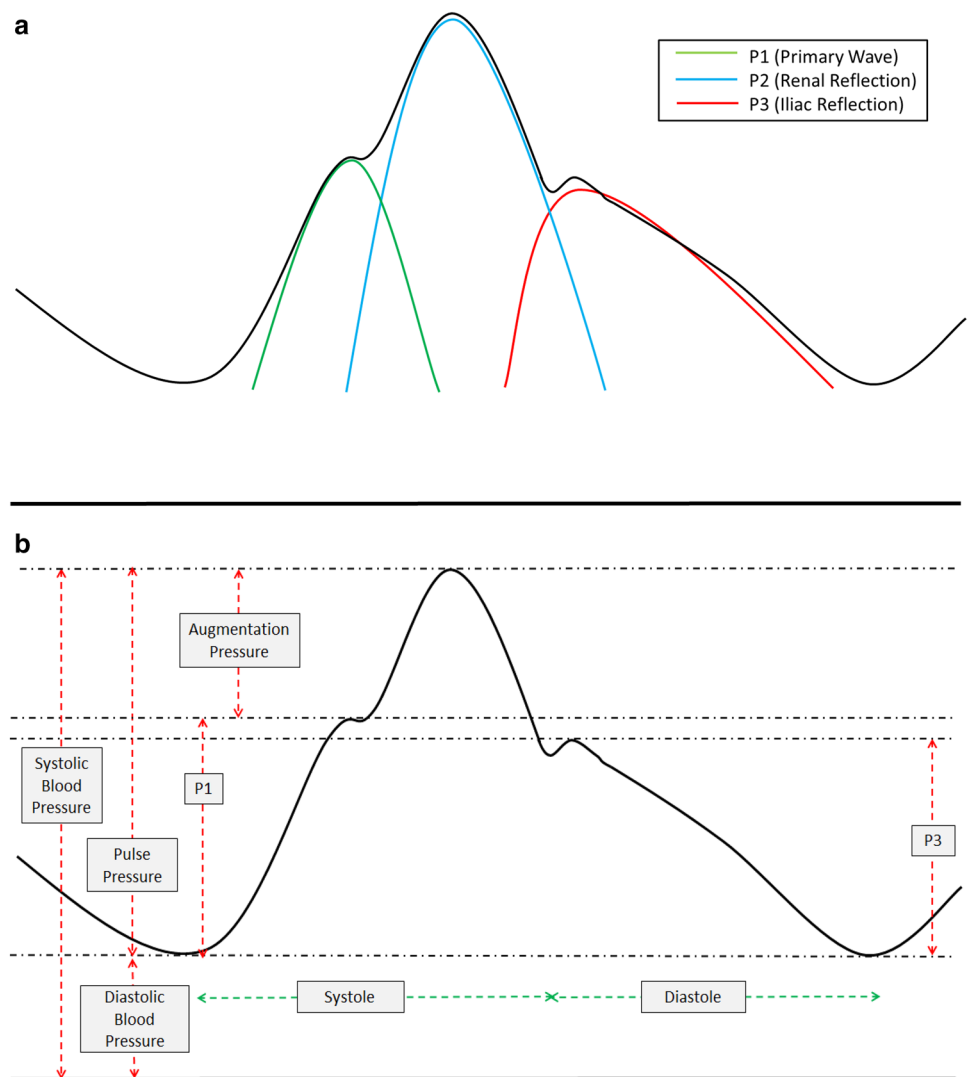
through conversion of a signal (the arterial waveform) as a function of time to a function of frequency. Various waves of differing frequencies and amplitudes are isolated through Fourier transform and are termed harmonics. The first harmonic (typically ranging between 1 and 2 Hz at baseline) represents heart rate and the amplitude (or power spectrum density) of the harmonic represents blood pressure. Higher frequency harmonics incorporate the phase and amplitude changes of the primary and reflected waves.

Conventional Fourier transform methodology analyzes the entire signal duration and, therefore, is limited in detecting and measuring dynamic changes (such as progressive hemorrhage). Short-time Fourier transform (STFT) is an alternative method that allows Fourier transform to be performed on multiple short segments and then the differences in frequency and amplitude of the harmonics can be compared across time. Analysis using STFT was utilized to characterize the changes in the frequency domain during progressive hemorrhage.

The variance of the harmonic frequency peak, as well as the variance of the harmonic power spectrum density, was calculated during hemorrhage for the first three harmonics. This was done to quantify short-term hemodynamic variability as a potential measure of instability and progressive hemorrhage. Linear and non-linear (sigmoidal) regression modeling were used to quantify trends and strength of associations between changes in variance during hemorrhage.

Regression diagnostics were performed to ensure that statistical assumptions regarding the models were valid. Normality was examined for variables using frequency histograms, box plots, and D'Agostino's omnibus normality test. Residual plots were computed and plotted to assess leverage and the influence of potentially influential data points and to determine whether the regression function was linear. The null hypothesis assumed that the overall slope of the line was zero, and where $p < 0.05$ on testing, the null hypothesis was rejected. Lack-of-fit testing to assess evidence of inadequate modeling using sigmoidal

regression was performed using the replicates test. Goodness-of-fit tests were also applied and the coefficients of determination were reported (R^2).

Results

Baseline characteristics

Ten animals were included. Two were male and eight female. The mean ± standard deviation (SD) weight (kg) was 80.8 ± 11.2. All animals tolerated the 40% exponential controlled hemorrhage without any animals having premature cessation of hemorrhage. The baseline and change after hemorrhage values for several hemodynamic and laboratory values are listed in Table 1. Mean (± SD) crystalloid resuscitation during the hemorrhage was 1297 ± 288 mL.

Effects of hemorrhage on hemodynamics and arterial pressure waveform morphomics

Upon successful induction into hemorrhage, the animals became hypotensive, as demonstrated in Fig. 2a. There was a plateau in blood pressures at approximately 20% hemorrhage. Individual arterial waveform features and indices were plotted and best fitting regression lines were superimposed (see Fig. 2b, c). Several features changed in a directly or inversely proportional manner to systolic and diastolic blood pressure, and plateaued around 20% hemorrhage. The best fitting regression modeling was non-linear sigmoid regression for all features, except the P1:P3 index, which was best fitted with linear regression (Table 2).

Table 1 Baseline and end of hemorrhage hemodynamic and laboratory parameters

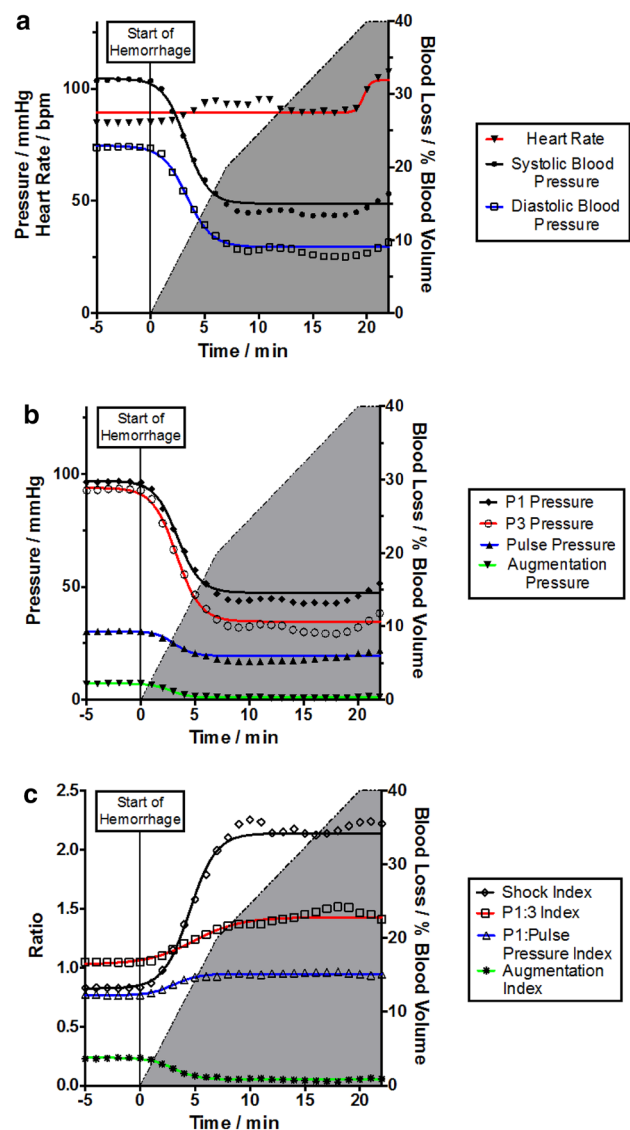| Parameters	Baseline	End of hemorrhage	p value
Physiology			
HR (BPM)	85 ± 17	105 ± 19	0.03
SBP (mmHg)	104 ± 16	50 ± 13	< 0.01
DBP (mmHg)	74 ± 16	29 ± 13	< 0.01
SpO$_2$ (%)	98.7 ± 2.6	94.4 ± 8.8	0.69
Lab index			
Hemoglobin (g/dL)	11.1 ± 1.4	8.4 ± 2.2	0.01
pH	7.45 ± 0.04	7.39 ± 0.09	0.01
Base excess	2.9 ± 1.6	− 0.2 ± 3.8	0.01
pO$_2$ (mmHg)	437 ± 87	443 ± 109	0.77
Lactate (mmol/L)	2.8 ± 1.4	4.6 ± 3.8	0.08

Fig. 2 Graphs demonstrating a number of hemodynamic parameters and blood loss against time. **a** Parameters that were measured directly during the experiments. **b** Parameters which were derived from signal processing of continuous blood pressure data. **c** Computed indices of derived values

Effect of hemorrhage on arterial waveform using the frequency domain and STFT

The changes in the arterial waveform were also analyzed through the frequency domain by STFT. A case example of the arterial waveform seen in the frequency domain by STFT is illustrated in Fig. 3a, b. The first (lowest) frequency trend line/harmonic is at approximately 1–2 Hz. Additional higher frequency harmonics can be seen at approximately 3–4 Hz, at 5–6 Hz, and 6–7 Hz. As observed in this example, the first three harmonics closely mirror each other, but are not identical, which is likely a result of the primary and reflected

Table 2 Linear and sigmoidal regression modeling for key hemodynamic features

Parameters	Linear regression R^2	p value	Sigmoidal regression R^2	Inadequate model?
SBP	0.42	< 0.01	0.74	No
DBP	0.47	< 0.01	0.69	No
Pulse pressure	0.11	< 0.01	0.49	No
Augmentation pressure	0.28	< 0.01	0.54	No
P1:P3 index	0.51	< 0.01	0.46	No
P1: pulse pressure index	0.24	< 0.01	0.38	No
Augmentation index	0.25	< 0.01	0.38	No
Shock index	0.20	< 0.01	0.34	No
Heart rate	< 0.01	0.83	0.01	No
P1 pressure	0.41	< 0.01	0.71	No
P3 pressure	0.49	< 0.01	0.76	No
Power spectrum density variance				
Harmonic 1	0.90	< 0.01	0.31	No
Harmonic 2	0.90	< 0.01	0.31	No
Harmonic 3	0.59	< 0.01	0.09	No
Frequency variance				
Harmonic 1	0.70	< 0.01	0.26	No
Harmonic 2	0.93	< 0.01	0.31	No
Harmonic 3	0.76	< 0.01	0.18	No

The strength of the models is reflected in the R^2 value

waves changing at different rates. In addition, Fig. 3a, b demonstrates relative stability at baseline, with minimal variance. During progressive hemorrhage the frequencies of the harmonics increase in a relatively linear fashion until approximately 10 min, where further hemorrhage starts to be associated with significant fluctuations/variance. Analysis of the first three harmonics during progressive hemorrhage, as seen in Fig. 3c, demonstrated increasing variance with high coefficients of determination using linear regression in frequency ($R^2 = 0.70$, 0.93, and 0.76, respectively) and power spectrum density ($R^2 = 0.90$, 0.90, and 0.59, respectively).

Discussion

The current study is a characterization of the changes observed in key features of the arterial waveform during an exponential, volume-controlled experimental hemorrhage model in swine. When assessing the component wave patterns, the primary wave (P1) was relatively preserved, while the renal (P2) and iliac (P3) wave reflections became noticeably attenuated. The blood pressure changed dramatically during the initial phase of hemorrhage, but plateaued at around 20% hypovolemia, limiting its ability to discriminate

between moderate and severe hemorrhage in this animal model.

More specific waveform features, extracted using signal-processing techniques were also examined, most of which demonstrated a sigmoidal relationship when modeled with hypovolemia against time. The only features to show a linear relationship was the P1:P3 ratio and the variance of the amplitude and frequency of the arterial waveform. The P1:P3 ratio had a weak association ($R^2 = 0.51$) with hypovolemia, so may be of limited clinical usefulness. The variance of blood pressure harmonics had a stronger association ($R^2 = 0.90$) and may be parameters of interest in assessing depth of hemorrhagic shock in trauma patients.

These findings conflict with some of the established concepts in hemorrhagic shock pathophysiology. The process of physiological compensation is well described, where subjects are able to maintain their blood pressure through vasoconstriction and tachycardia, until these mechanisms are overcome resulting in hypotension. However, the hemodynamic response to hemorrhage appears to be significantly affected by the rate of bleeding, something which is poorly recognized in clinical practice. The physiological response observed in the current study reflects the process of rapid exsanguination, where hypotension appears to be an early and dominant feature.

Previous investigators have examined various rates of continuous, controlled hemorrhage and demonstrated that exponential hemorrhage leads to more profound tachycardia and hypotension, with a greater ischemic burden and depth of shock [13]. In addition, early and acute hypotension has been similarly reported by other animal studies using the same hemorrhage protocol as the current study [15]. Other recent swine models of severe uncontrolled hemorrhage in solid organ injury and vascular injury have demonstrated an acute, rapid, and immediate decrease in blood pressure upon the initiation of bleeding [16–18].

The applicability of swine studies to human physiology is imperfect as there are differences; the swine is a prey animal which has specific adaptations to mitigate hemorrhage, such as a large contractile spleen [17]. However, it is difficult to study rapid hemorrhage in human subjects in a controlled manner. The two established methods only simulate moderate hemorrhage and include lower body negative pressure chambers and controlled venesection [19, 20]. Both techniques use progressive, slow, step-wise reductions in blood volume with periods of rest or equilibration between further removal of volume [11, 20–22]. These slow and intermittent hemorrhage protocols lead to relative hemodynamic stability during progressive hemorrhage with hypotension and tachycardia appearing only as a late finding.

A fundamental consideration not addressed by these studies is that some traumatic injuries present as rapid exsanguination, and the hemodynamic response may result in an

Fig. 3 Short-time Fourier transform analysis. **a, b** A case illustration of Fourier transform of the arterial waveform at baseline, during progressive hemorrhage (from H_0 to 20 min), and immediately after hemorrhage (20–30 min). **a** A two-dimensional representation, and **b** a three-dimensional representation. **c** The frequency and power spectrum density variance during progressive hemorrhage for each of the first three harmonics
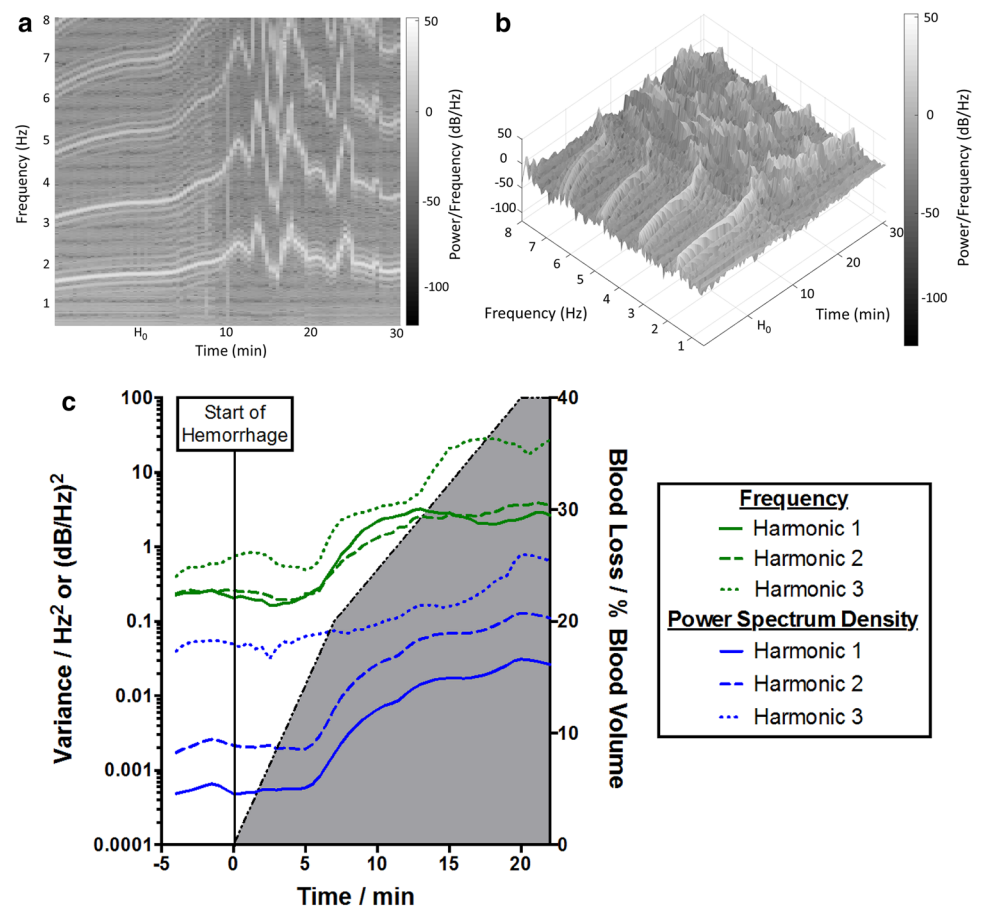
early rapid decrease in blood pressure. In fact, in the setting of severe hemorrhage, it may be advantageous to use hypotension as a beneficial compensatory mechanism to mitigate ongoing hemorrhage.

The ability to better identify patients in severe hemorrhagic shock may help to expedite precision interventions, leading to improved outcomes. Endovascular resuscitation and hemorrhage control maneuvers are being increasingly used in contemporary practice, with early arterial access proving to be the critical first step [23]. Not only does this permit vascular access, but it also allows for beat-to-beat monitoring and interrogation of the waveform morphomics. This type of waveform analysis and hemorrhage-severity assessment may be useful in the setting of an increasing prevalence of arterial line monitoring in patients who are moderately to severely injured.

The potential utility of using arterial waveform morphomics to distinguish between severities of hemorrhage is likely rooted in the physiologic basis of these wave components. Stroke volume, cardiac contractility, arterial capacitance, intra-arterial volume, vasoconstriction, systemic vascular resistance, and arterial compliance are among the many physiological factors that likely influence the timing and amplitude of these arterial waveform

components. Other factors to consider include variations in anatomy (e.g., angle of branch vessel origins), comorbidities (e.g., calcific atherosclerotic burden), trauma (e.g., location of hemorrhagic focus) and iatrogenic issues (e.g., other arterial catheters or tourniquets). We hypothesize that the relative preservation of the primary wave (P1) represents a preservation of cardiac function and output, while the diminution of the reflective waves (P2 and P3) represents decreased aortic pulsatility as a function of intra-arterial volume depletion.

Intra-arterial volume depletion and decreased aortic pulsatility during hemorrhagic shock have been previously demonstrated in swine models, and intra-arterial volume depletion during severe hemorrhagic shock has been previously described in humans [24–27]. Importantly, a previous study using swine has demonstrated that these waveform features are restored upon blood transfusion and resuscitation after hemorrhagic shock [10]. In addition, a study in humans using a lower body negative pressure chamber to induce central hypovolemia found similar waveform feature changes that were reversed upon reversal of central hypovolemia [9]. These findings support the hypothesis that these features are a function of intra-arterial volume depletion and decreased pulsatility.

Increasing variance of the cardiovascular system are likely a strong indicator of the instability of the biological system (the swine) and impending decompensation/collapse. As seen in Fig. 3, differences in variance of both frequency and power spectrum density (heart rate and blood pressure) progressively changed with continued hemorrhage. The calculation of frequency and power spectrum density variance using STFT from the arterial waveform provides a powerful potential tool in the ability to distinguish differing severities of hemorrhage. We suspect that proprietary machine-learning algorithms, which incorporate multiple features of the arterial waveform to predict clinical decompensation, may also use measures of system instability such as variance [20, 28]. Additional investigations are required to better characterize measures of hemodynamic system instability during hemorrhage as well as the response to resuscitation.

Importantly, while the currently study has focused on invasive arterial blood pressure measurements, there are other physiological measurements where the same type of Fourier analysis can be applied. There is a longstanding and validated use of heart rate variability in the obstetric literature, which has also been evaluated in hemorrhage [29]. Similarly, techniques like the Brain Acoustic Monitor combines signal waveform data and the acoustic signature of brain parenchyma within a time domain to produce an index that reflects brain injury [30]. These kinds of sensors have the advantage that they are non-invasive, widening their clinical availability to areas such the pre-hospital environment [31].

This study has several limitations that are important to discuss. First, the animals retained their spleens, which may have contributed red cell mass to the animals' circulation during the later stages of the hemorrhage. This concept, however, is controversial in swine hemorrhage modeling, with some investigators of a view that the spleen contributes little in the acute phase of hemorrhage [32].

Second is the use of crystalloid transfusion during the hemorrhage phase. The use of synthetic fluid was considered necessary for the next phase of experiments, but can clearly confound the results by changing both intravascular volume and hemoglobin concentration—all linked to oxygen delivery. As the criteria for administration was subjective, rather than objective, it is particularly difficult to control for this in the analyses. Interestingly, the blood pressure performance reported in the current study appears similar to published results observed with fluid-naïve animals.

The need for additional fluid may also signal that the model was overly aggressive, with the appearance of early hypotension. This provokes questions about the clinical relevance of this model and the application of the analyses. Fundamentally, hypotension is a key piece of clinical data on which to initiate hemorrhage control maneuvers (tourniquet, laparotomy, etc.) and a morphomics analysis will

not change this paradigm. The current study demonstrates a principle which may have utility, but should be explored further. Future research should focus on quantifying the changes in arterial waveform morphomics in hemorrhage models with different depth and rates of hemorrhage, in fluid-naïve animals.

Finally, animals in this model were anesthetized in accordance with accepted best ethical practices. Hence, the physiological changes observed in this study may not be externally generalizable to actual human trauma patients who are not anesthetized. Non-anesthetized animals or humans might exhibit different physiological responses, such as compensatory vasoconstriction in the absence of vasodilating anesthetic agents (i.e., propofol and volatile anesthetics).

Conclusions

In this swine model of volume-controlled hemorrhage, hypotension was a predominant early feature. This may relate to porcine physiology, or a phenomenon that relates to the rate of hemorrhage. While most waveform features mirrored those of BP, specific features such as the variance of blood pressure harmonics, derived using signal processing and Fourier transform analysis, may be able to distinguish differing magnitudes of hemorrhage despite little change in conventional measures.

Compliance with ethical standards

Conflict of interest Philip J. Wasicek declares that he has no conflict of interest. William A. Teeter declares that he has no conflict of interest. Shiming Yang declares that he has no conflict of interest. Peter Hu declares that he has no conflict of interest. William B. Gamble declares that he has no conflict of interest. Samuel M. Galvagno declares that he has no conflict of interest. Melanie R. Hoehn declares that he has no conflict of interest. Thomas M. Scalea declares that he has no conflict of interest. Jonathan J. Morrison declares that he has no conflict of interest.

Ethical approval All applicable international, national, and/or institutional guidelines for the care and use of animals were followed. All the procedures performed in the current study that involved animals were in accordance with the ethical standards of the institution (University of Maryland) at which the current study was conducted.

References

1. Morrison JJ. Noncompressible torso hemorrhage. Crit Care Clin. 2017;33(1):37–54. https://doi.org/10.1016/j.ccc.2016.09.001.

2. Kisat M, Morrison JJ, Hashmi ZG, Efron DT, Rasmussen TE, Haider AH. Epidemiology and outcomes of non-compressible torso hemorrhage. J Surg Res. 2013;184(1):414–21. https://doi.org/10.1016/j.jss.2013.05.099.

3. Stannard A, Morrison JJ, Scott DJ, Ivatury RA, Ross JD, Rasmussen TE. The epidemiology of noncompressible torso hemorrhage in the wars in Iraq and Afghanistan. J Trauma Acute Care Surg. 2013;74(3):830–4. https://doi.org/10.1097/TA.0b013e31827a3704.

4. ATLS Subcommittee, American College of Surgeons' Committee on Trauma, International ATLS working group. Advanced trauma life support (ATLS®): the ninth edition. J Trauma Acute Care Surg. 2013;74(5):1363–6. https://doi.org/10.1097/ta.0b013e31828b82f5.

5. Guly HR, Bouamra O, Spiers M, Dark P, Coats T, Lecky FE. Vital signs and estimated blood loss in patients with major trauma: testing the validity of the ATLS classification of hypovolaemic shock. Resuscitation. 2011;82(5):556–9. https://doi.org/10.1016/j.resuscitation.2011.01.013.

6. Guly HR, Bouamra O, Little R, et al. Testing the validity of the ATLS classification of hypovolaemic shock. Resuscitation. 2010;81(9):1142–7. https://doi.org/10.1016/j.resuscitation.2010.04.007.

7. Mutschler M, Hoffmann M, Wölfl C, et al. Is the ATLS classification of hypovolaemic shock appreciated in daily trauma care? An online-survey among 383 ATLS course directors and instructors. Emerg Med J. 2015;32(2):134–7. https://doi.org/10.1136/emermed-2013-202727.

8. Mutschler M, Nienaber U, Brockamp T, et al. A critical reappraisal of the ATLS classification of hypovolaemic shock: does it really reflect clinical reality? Resuscitation. 2013;84(3):309–13. https://doi.org/10.1016/j.resuscitation.2012.07.012.

9. Baruch MC, Warburton DE, Bredin SS, Cote A, Gerdt DW, Adkins CM. Pulse decomposition analysis of the digital arterial pulse during hemorrhage simulation. Nonlinear Biomed Phys. 2011;5(1):1. https://doi.org/10.1186/1753-4631-5-1.

10. Dark P, Little R, Nirmalan M, Purdy J. Systemic arterial pressure wave reflections during acute hemorrhage. Crit Care Med. 2006;34(5):1497–505. https://doi.org/10.1097/01.CCM.0000215451.26971.89.

11. Convertino V, Grudic G, Mulligan J, Moulton S. Estimation of individual-specific progression to impending cardiovascular instability using arterial waveforms. J Appl Physiol. 2013;115(8):1196–202. https://doi.org/10.1152/japplphysiol.00668.2013.

12. Kilkenny C, Browne WJ, Cuthill IC, Emerson M, Altman DG. Improving bioscience research reporting: the arrive guidelines for reporting animal research. PLoS Biol. 2010;8(6):e1000412. https://doi.org/10.3390/ani4010035.

13. Frankel DAZ, Acosta JA, Anjaria DJ, et al. Physiologic response to hemorrhagic shock depends on rate and means of hemorrhage. J Surg Res. 2007;143(2):276–80. https://doi.org/10.1016/j.jss.2007.01.031.

14. Latham RD, Westerhof N, Sipkema P, Rubal BJ, Reuderink P, Murgo JP. Regional wave travel and reflections along the human aorta: a study with six simultaneous micromanometric pressures. Circulation. 1985;72(6):1257–69. https://doi.org/10.1161/01.CIR.72.6.1257.

15. Morrison JJ, Ross JD, Markov NP, Scott DJ, Spencer JR, Rasmussen TE. The inflammatory sequelae of aortic balloon occlusion in hemorrhagic shock. J Surg Res. 2014;191(2):423–31. https://doi.org/10.1016/j.jss.2014.04.012.

16. Morrison JJ, Ross JD, Houston R, Watson JDB, Sokol KK, Rasmussen TE. Use of resuscitative endovascular balloon occlusion of the aorta in a highly lethal model of noncompressible torso hemorrhage. Shock. 2014;41(2):130–7. https://doi.org/10.1097/SHK.0000000000000085.

17. Ross JD, Burns CJ, Sagini EM, Zarzabal LA, Morrison JJ. A laparoscopic swine model of noncompressible torso hemorrhage. J Trauma Acute Care Surg. 2014;77(3 Suppl. 2):77–82. https://doi.org/10.1097/TA.0000000000000385.

18. Morrison JJ, Percival TJ, Markov NP, et al. Aortic balloon occlusion is effective in controlling pelvic hemorrhage. J Surg Res. 2012;177(2):341–7. https://doi.org/10.1016/j.jss.2012.04.035.

19. Cooke WH, Ryan KL, Convertino VA. Lower body negative pressure as a model to study progression to acute hemorrhagic shock in humans. J Appl Physiol. 2004;96(4):1249–61. https://doi.org/10.1152/japplphysiol.01155.2003.

20. Convertino VA, Howard JT, Hinojosa-Laborde C, et al. Individual-specific, beat-to-beat trending of significant human blood loss: the compensatory reserve. Shock. 2015;44(8):27–32. https://doi.org/10.1097/SHK.0000000000000323.

21. Convertino VA, Cooke WH, Holcomb JB. Arterial pulse pressure and its association with reduced stroke volume during progressive central hypovolemia. J Trauma Inj Infect Crit Care. 2006;61(3):629–34. https://doi.org/10.1097/01.ta.0000196663.34175.33.

22. Janak JC, Howard JT, Goei KA, et al. Predictors of the onset of hemodynamic decompensation during progressive central hypovolemia. Shock. 2015;44(6):548–53. https://doi.org/10.1097/SHK.0000000000000480.

23. Romagnoli A, Teeter W, Pasley J, et al. Time to aortic occlusion: it's all about access. J Trauma Acute Care Surg. 2017;83(6):1161–4. https://doi.org/10.1097/TA.0000000000001665.

24. Jonker FHW, Mojibian H, Schlösser FJV, et al. The impact of hypovolaemic shock on the aortic diameter in a porcine model. Eur J Vasc Endovasc Surg. 2010;40(5):564–71. https://doi.org/10.1016/j.ejvs.2010.07.014.

25. Jonker F, van Keulen J, Schlosser F, et al. Thoracic aortic pulsatility decreases during hypovolemic shock: implications for stent-graft sizing. J Endovasc Ther. 2011;18(4):491–6. https://doi.org/10.1583/10-3374.1.

26. Jonker FHW, Verhagen HJM, Mojibian H, Davis K, Moll FL, Muhs BE. Aortic endograft sizing in trauma patients with hemodynamic instability. J Vasc Surg. 2010;52(1):39–44. https://doi.org/10.1016/j.jvs.2010.02.256.

27. Wasicek PJ, Shanmuganathan K, Yang S, Scalea TM, Brenner ML. Effect of severe traumatic hemorrhage on large arterial diameter as determined by computed tomography (CT). J Endovasc Resusc Trauma Manag. 2018;2(1):23–9. https://doi.org/10.26676/jevtm.v2i1.45.

28. Moulton SL, Mulligan J, Grudic GZ, Convertino V. Running on empty? The compensatory reserve index. J Trauma Acute Care Surg. 2013;75(6):1053–9. https://doi.org/10.1097/ta.0b013e31828aa811a.

29. Cooke WH, Salinas J, Convertino VA, Ludwig DA, Hinds D, Duke JH, Moore FA, Holcomb JB. Heart rate variability and its association with mortality in prehospital trauma patients. J Trauma. 2006;60(2):363–70.

30. Dutton RP, van der Heijden M, Aarabi BA, Sewell J, Scalea TM. Screening TBI patients with the brain acoustic monitor: association with CT scan findings and neurologic status at hospital discharge. Clin Intensive Care. 2005;16:97–105.

31. Mackenzie CF, Wang Y, Hu PF, Chen SY, Chen HH, Hagegeorge G, Stansbury LG, Shackelford S. Automated prediction of early blood transfusion and mortality in trauma patients. J Trauma Acute Care Surg. 2014;76(6):1379–85.

32. Boysen SR, Caulkett NA, Brookfield CE, Warren A, Pang JM. Splenectomy versus sham splenectomy in a swine model of controlled hemorrhagic shock. Shock. 2016;46(4):439–46. https://doi.org/10.1097/SHK.0000000000000608.